Journal of Air-Conditioning and Refrigertion Volume 7 September (1999) / pp. 1~10

A Study of Ice-Formation Phenomena on Freezing of Flowing Water in a Stenotic Tube

Jeong-Se Suh*, Moo-Geun Kim**, Sung Tack Ro*** and Chang Soon Yim****

Key Words: Ice-Formation, Stenotic Tube, Phase-Change, Laminar Flow

Abstract

In this study, a numerical analysis is made on the ice-formation for laminar water flow inside a stenotic tube. The study takes into account the interaction between the laminar flow and the stenotic port in the circular tube. The purpose of the present numerical investigation is to assess the effect of a stenotic shape on the instantaneous shape of the flow passage during freezing upstream/downstream of the stenotic channel. In the solution strategy, the present study is substantially distinguished from the existing works in that the complete set of governing equations in both the solid and liquid regions are resolved. In a channel flow between parallel plates, the agreement befween the of predictions and the available experimental data is very good. Numerical analyses are performed for parametric variations of the position and heights of stenotic shape and flow rate. The results show that the stenotic shape has the great effect on the thickness of the solidification layer inside the tube. As the height of a stenosis grows and the length of a stenosis decreases, the ice layer thickness near the stenotic port is thinner, due to backward flow caused by the sudden expansion of a water tunnel. It is found that the flow passage has a slight uniform taper up to the stenotic channel, at which a sudden expansion is observed. It is also shown that the ice layer becomes more fat in accordance with its Reynolds number.

* Dept. of Mechanical Engineering, Gyeongsang National University, Chinju 660-701, Korea
** Dept. of Mechanical Engineering, Inje University, Kimhae 621-749, Korea
*** Dept. of Mechanical Engineering, Seoul National University, Seoul 151-742, Korea
**** Dept. of Mechanical Engineering, Inha University, Inchon 402-751, Korea

Nomenclature

c : heat capacity [J · kg^{-1} · °C^{-1}]
D : diameter of tube [m], $2R$
H : one-half length of distance between two plates [m]
hc : heat transfer coefficient [W · m^{-2} · °C^{-1}]
k : thermal conductivity [W · m^{-1} · °C^{-1}]
L : length of tube [m]
Nu : Nusselt number, $h_c D/k$
p : pressure [Pa]
Pr : Prandtl number, ν/α_L
R : radius of tube [m]
Re : Reynolds number, $u_{m,i} D/\nu$
T_i : inlet temperature of water [°C]
T_f : freezing temperature [°C]
T_w : wall temperature of tube [°C]
u, v : velocity components in x, r directions [m · s^{-1}]
u_i : inlet velocity of tube [m · s^{-1}]
$u_{m,i}$: inlet mean velocity of tube [m · s^{-1}]
x, r : cylindrical coordinates in an axial/ radial direction [m]

Greek symbols

α : thermal diffusivity [m^2 · s^{-1}]
Δ_s : freezing layer thickness in a center of stenotic port [m]
δ_i : radius of tube to the ice layer [m]
θ : dimensionless temperature, Eq.(10)
λ_s : one-half of axial length of stenotic port [m]
ν : kinematic viscosity [m^2 · s^{-1}]
ξ, η : transformed coodinate system
ρ : density [kg · m^{-3}]

Subscripts

i : inlet
s : stenosis

1. Introduction

The freezing phenomena of internal liquid flow take place commonly in many diverse processes and situations which involve water-freezing in pipes, the blockage of chemical process lines, and the freezing of liquid metals in a heat exchanger. In many of these, freezing may have undesirable effects. Whether freezing is desirable or undesirable, it is imperative that the basic freezing phenomena and heat transfer characteristics in pipe freezing flows be understood.

The study on the freezing problem in a pipe was set forth by Zerkle and Sunderland[1] to account for freezing of a liquid in a pipe due to the step change in the pipe wall temperature. Since then, a number of investigations has been performed theoretically and experimentally to study freezing flows in a circular tube and parallel plate channels and its effect upon heat transfer. A survey of the literatures shows that the studies on the freezing of pipe flow have been classified into two types, One such type [1-4] is to obtain the information on freezing in laminar flow and the other[5-9] in turbulent flow. In the case of laminar flow, the freezing layer is thickly formed near the pipe wall and thus affects the flow characteristics through the pipeline[8]. In the treatment of solidification in turbulent flow, the increase in the ice layer thickness along the axial direction is very small, so that it does not affect the flow characteristics[9]. However, there is an interaction between the turbulent flow and the shape of the ice at

the ice-water interface if the ice layer is not thin. This interaction results in an instability in the ice layer. A wavy ice structure appears in the entrance region of the cooled pipe due to the instability caused by a strong laminarization of the turbulent flow. As discussed earlier, it is clear that for a laminar flow the increase in the thickness of ice layer has a great effect on the flow characteristics in the channel. As a result, many investigations have been focused on the thickness of ice layer in laminar flow in channel. However, all of the preceding investigations concern the freezing in constant-area straight ducts installed horizontally or vertically. In a freezing problem in a channel, if the flow channel has a stenotic port such as a sediment, a valve, a coupler of pipe, and so forth, the shape of ice layer formed on the pipe wall is expected to substantially distinguish from that in a straight pipeline. In specific, the flow patterns are suddenly varied upstream and downstream of the stenotic port. Due to such a flow structure, the sudden variation of ice layer thickness in the vicinity of the stenosis will be observed.

In this study, a numerical analysis is made for the freezing phenomena in a stenotic tube for a steady state laminar flow. The purpose of the present investigation is to assess the effect of the stenotic port on the shape of the flow passage. The present study is markedly different from the existing works in that the complete set of governing equations in both the solid and liquid regions are resolved. The numerical analysis is performed for various position and heights of stenotic shape and flow rates.

2. Analysis

2.1 Physical description and basic equations

Figure 1 illustrates a typical configuration of the ice-water system for the freezing phenomena in a cylindrical tube of diameter D. The wall temperature of a tube is maintained at a uniform constant temperature T_w which is lower than the freezing temperature T_f. The fluid which has a uniform temperature $T_i (> T_f)$ and a fully developed velocity u_i enters into the circular tube. At the inlet x=0, the cooling begins and the frozen layer is formed on the wall as the fluid proceeds through the pipe line. Several idealizations are introduced for the analysis: (1) the melting process is two- dimensional and axisymmetric with respect to the centerline of pipe; (2) the Newtonian liquid and the laminar flow are assumed; and (3) the thermophysical properties are constant.

A general conser vation equation(10) is written in the Cartesian coordinate as:

$$\frac{\partial}{\partial x}\left(r\rho u\phi - r\Gamma\frac{\partial\phi}{\partial x}\right)+\frac{\partial}{\partial r}\left(r\rho v\phi - r\Gamma\frac{\partial\phi}{\partial r}\right) = rS(x, r) \tag{1}$$

which is repeated for the continuity, momentum, energy equations in the liquid phase; and for the energy equation in the solid phase. Next, transformation of the coordinate is performed for the governing equation (1) using

$$x = x(\xi,\ \eta), \qquad r = r(\xi,\ \eta) \tag{2}$$

which yields

$$\frac{\partial}{\partial\xi}\left(\rho U\phi - \frac{\alpha_\xi\Gamma}{h_\xi}\frac{\partial\phi}{\partial\xi}\right)+\frac{\partial}{\partial\eta}\left(\rho V\phi - \frac{\alpha_\eta\Gamma}{h_\eta}\frac{\partial\phi}{\partial\eta}\right) = JS(\xi,\eta) - \frac{\partial}{\partial\xi}\left(\frac{\beta_\xi\Gamma}{h_\eta}\frac{\partial\phi}{\partial\eta}\right) - \frac{\partial}{\partial\eta}\left(\frac{\beta_\eta\Gamma}{h_\xi}\frac{\partial\phi}{\partial\xi}\right) \tag{3}$$

where

$$\alpha_\xi = r h_\xi h_\eta^2/J,\ \alpha_\eta = r h_\eta h_\xi^2/J,\ \beta_\xi = r\lambda h_\eta/J,$$

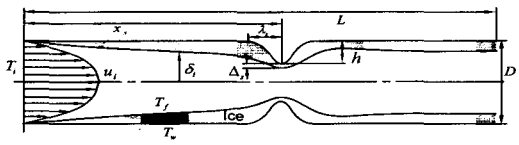

Fig.1 Schematic representation of the physical model for the ice-formation in a stenotic tube.

Table 1 Variables in the dimensionless governing equation

	ϕ^*	Γ^*	S^*
Solid	θ_S	$(k_r/c_r)(\mathrm{RePr})^{-1}$	0
Liquid	1	0	0
	u^*	Re^{-1}	$-\partial p^*/\partial x^*$
	v^*	Re^{-1}	$-\partial p^*/\partial r^* - \mathrm{Re}^{-1}v^*/r^{*2}$
	θ_L	$(\mathrm{RePr})^{-1}$	0

$$\beta_\eta = r\lambda h_\xi/J,\quad h_\xi=(x_\xi^2+r_\xi^2)^{1/2},\quad h_\eta=(x_\eta^2+r_\eta^2)^{1/2},$$
$$\lambda = x_\xi x_\eta + r_\xi r_\eta,\quad J = x_\xi r_\eta - r_\xi x_\eta,\quad \hat{J}=rJ$$

and other factors appearing in the above transformed equations are available in ref (11). The covariant velocity components are selected as the main dependent variables in solving the momentum equations following Karki and Patankar[12].

The interfacial conditions as follow are the temperature equilibrium, the conservation of the mass, energy fluxes crossing the moving interface and no-slip at the surface of the ice layer.

$$T_L = T_S = T_f \tag{4}$$

$$(\rho V)_L = (\rho V)_S \tag{5}$$

$$\left(\rho V\phi - \frac{a_\eta \Gamma}{h_\eta}\frac{\partial \phi}{\partial \eta}\right)_L = \left(\rho V\phi - \frac{a_\eta \Gamma}{h_\eta}\frac{\partial \phi}{\partial \eta}\right)_S \tag{6}$$

$$u = v = 0 \tag{7}$$

where ϕ denotes the entalphy of solid and liquids at the interface.

The additional boundary conditions for the velocity and temperature are given as follow: The thermal boundary conditions are the adiabatic conditions at the lines of symmetry; the constant temperature conditions at the wall and at the interface; and for the velocity fields, zero-shear and impermeable surface are assumed at the lines of symmetry; no-slip is imposed at the wall.

$$T_S = T_w \quad \text{at the wall of pipe} \tag{8}$$

$$\frac{\partial u}{\partial r} = v = 0,\quad \frac{\partial T}{\partial r} = 0 \quad \text{at the symmetric line} \tag{9}$$

To facilitate the analysis, the dimensionless group of parameters are introduced as follow:

$$x^* = \frac{x}{D},\quad r^* = \frac{r}{D},\quad u^* = \frac{u}{u_{m,i}},\quad v^* = \frac{v}{u_{m,i}},$$
$$p^* = \frac{p}{\rho_L u_{m,i}^2},\quad \mathrm{Re} = \frac{u_{m,i}D}{\nu},\quad \mathrm{Pr} = \frac{\nu}{a_L},$$
$$c_r = \frac{c_S}{c_L},\quad k_r = \frac{k_S}{k_L},\quad \theta_S = \frac{c_r(T_S - T_f)}{T_i - T_f},$$
$$\theta_L = \frac{T_L - T_f}{T_i - T_f}. \tag{10}$$

Using the dimensionless parameters, the entire set of governing equations in the solid and liquid phases can be rendered dimensionless, as summarized in Table 1.

In this study, the shape of a stenotic port is based on the cosine curve, which has been treated as a typical shape of stenosis in the representative literature[12], as follows:

$$r = \frac{D}{2} - h[1+\cos\{\pi(x-x_s)/\lambda_s\}] \qquad (x_s-\lambda_s \le x \le x_s+\lambda_s) \tag{11}$$

where each of δs, λs and xs is the radius of the tube in a center of stenotic port. One half of the axial length of stenotic port, and the axial

length between the inlet and stenosis positions, as shown in Fig.1.

2.2 Solution Procedure

After a number of grid resolutions were tried, a nonuniform grid system was constructed by deploying 71 nodes in the ξ-direction and 23 nodes in the η-direction. Using the equations as follows:

$$x = L\xi \quad (0 \le \xi \le 1)$$
$$r = \begin{cases} \delta_i \eta & (0 \le \eta < 1) \\ \delta_i + (\eta - 1)(R - \delta_i) & (1 \le \eta \le 2), \end{cases} \tag{12}$$

each of grid points in the physical domain corresponds to that in the computational domain. Near wall regions and in the vicinity of the interface, grids were densely distributed to accommodate the expected large gradient of the field variables.

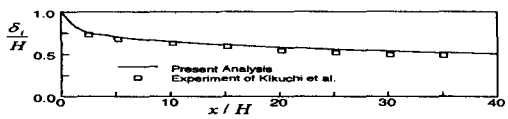

Fig.2 The shapes of the interface for steady state freezing of liquid in laminar flow between two parallel plates in T_w= -1.2℃, T_i= 2℃, $u_{m,i}\, H/\nu = 175$ Experimental results from ref. (3) (rectangular) and Numerical results from this study (solid lines).

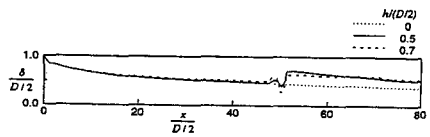

Fig.3 Ice formation layer for the smooth and stenotic tubes.

The coupling between the continuity and the momentum equations are resolved via the SIMPLER algorithm [10]. The interface movement was implicitly treated and the overall energy balance was satisfied to within a tolerance of 0.01%.

3. Results and Discussion

The research purpose in this study is to investigate the effect of the stenosis on the freezing layer thickness for laminar flow in a stenotic tube. Therefore, the results from calculation is mainly to be presented for the variation of freezing layer thickness under these conditions; the shape and position of stenosis; the intensity of velocity; the wall temperature of tube; and the inlet temperature of water. The calculations were carried out for the wall temperature $T_w = -2°C$ and the inlet temperature of water $T_i = 5°C$, All the results presented in this study have been verified for the range of laminar flow, $2\, u_m \delta\, i/\nu < 2100$.

At first, for the validity of the numerical procedures used in the present study, the calculated results from this study are compared with the experimental data reported by Kikuchi et. al[3] in the parallel channel flow as shown in Fig.2. The agreement between the numerical and the experimental data is very good.

3.1 Effects of the stenotic height

Figure 3 exhibits the shapes of the ice layer for a straight tube ($h = 0$) and stenotic tubes ($h = 0.25D$, $0.35D$), where the dotted line represents the straight tube, and the solid and dashed lines represent the stenotic tubes of $h = 0.25D$ and $h = 0.35D$. As shown in Fig.3, the

ice layer thickness monotonically increases in the axial direction for the straight tube. It is observed that the growth rate of ice layer is higher at the entrance of the tube than the tube downstream. This behavior is due to a hydrodynamical and thermal development of the fluid flow at the entrance of the tube. On the other hand, for stenotic tubes ($h=0.25D$, $0.35D$) the ice growth thickness before the stenotic port corresponding to $x_s=25D$ is about the same as that of the straight pipe, while the ice shape behind the stenotic port is markedly different. The ice layer thickness drop sharply right after the stenotic port. This decrease in the ice layer thickness for $h=0.35D$ is greater than for $h=0.25D$. This behavior may be caused by the interaction between the ice layer and the flow field in the liquid region. he fluid flow and temperature distributions with the ice layer thickness in the liquid region are displayed in Fig.4. In each figure, the isothermal lines in the liquid region are plotted above the axisymmetric line of the tube and the stream lines below the tube center line. For the straight tube depicted in Fig.4(a), the water entering the inlet of tube flows more rapidly as the flow passes downward. This is due to the reduction of the cross-sectional area of flow passage caused by the ice growth. For the temperature field in the liquid, an investigation for isothermal lines reveals that a thermal boundary layer is formed in the vicinity of the ice layer and gradually grows in the axial direction. From these flow patterns and temperature distributions, the monotonic increasing for the ice layer pattern in the straight pipeline can be deduced. On the other hand, for the stenotic tube of $h=0.25D$, the pattern for the flow and temperature fields before the stenotic port ($x_s=25D$) is about the same as for the straight pipeline. However, the vorticity of the flow occurs downstream of the stenotic port due to the steep expansion of the cross-sectional area. An investigation for Fig.4 (b) reveals that a thermal boundary layer is partially separated from the ice wall just behind the stenotic port, but mostly adhering closely to the ice layer.

This finding implies that the thermal boundary layer thickness is thin just behind the stenotic port. This same behavior for the flow and temperature patterns as in Fig.4(b) is read-

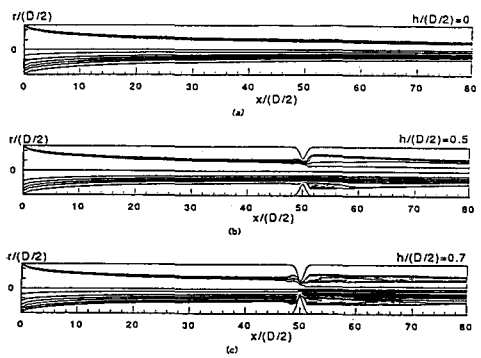

Fig.4 Contour plots for isotherms (upper) and stream lines (lower) : (a) $h=0$, (b) $h=0.25D$, (c) $h=0.35D$.

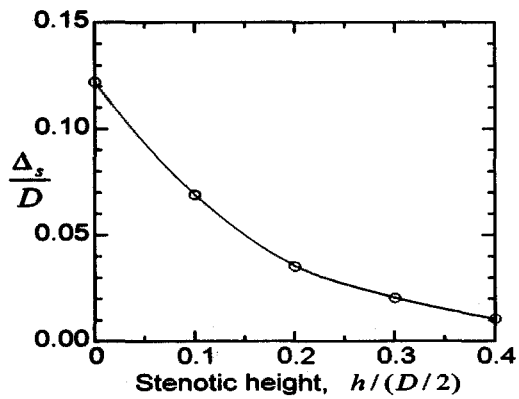

Fig.5 Variation of the ice layer thickness at the center of stenosis with several heights of stenosis.

ily observed in Fig.4(c) for the higher stenotic height of $h=0.35D$. Especially, the structure of recirculation is more complex and unstable .with the increasing height of the stenotic port. The recirculation cells are sequentially built up along the ice layer and some of them are stretched over the flow passage. These vortex cells enhance the heat transfer rate at the ice-water interface and lead to the extension of the thin ice layer behind the stenotic port. The shape pattern of the ice layer can be also found in Fig.3. And also, for the investigation of the effect of the stenosis height on the thickness of ice layer, the variation trend of ice layer thickness at the center portion of stenosis is depicted in Fig.5. In this figure, as the height of stenosis is increased, the ice layer thickness formed herin gets thinner monotonically. Such phenomena for an ice layer are arised from the fact that the increasing of temperature gradient is caused by the rapid variation of radial gradient of velocity and thus inhibits the growth of ice layer herein.

In addition, it is shown in Fig.6 that the length of stenotic portion influences the ice layer thickness. As shown in this figure, the thickness of ice layer gets thinner monotonically with the decreasing of the length of stenotic portion. A tendency of ice layer thickness is varied convexly, which is different from a variety of stenotic heights.

3.2 Effects of Reynolds number

Figure 7 shows the effect of flow intensity on the ice layer thickness in the axial direction for Re=100, 1000 and 2000. In this figure, for Re=100, the growth of ice layer monotonically increases in the axial direction and the shape of ice layer thickness is in contrast to those for other Reynolds numbers. It is observed that the ice layer thickness does not fluctuate in the vicinity of the stenotic section. However, for the higher Reynolds number of Re=2000, the ice layer thickness near the stenotic section is thinner than for Re=1000, except

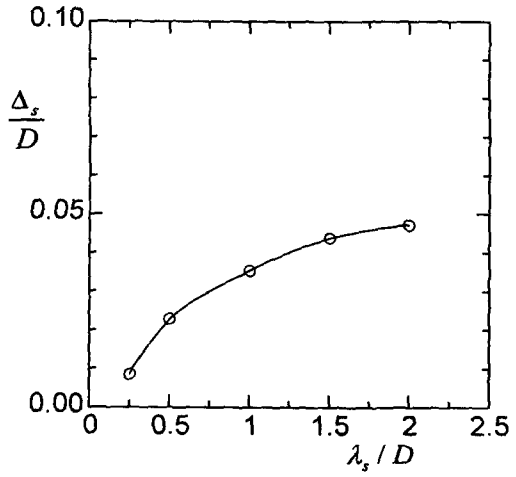

Fig.6 Variation of the ice layer thickness at the center of stenosis with various base lengths of stenosis.

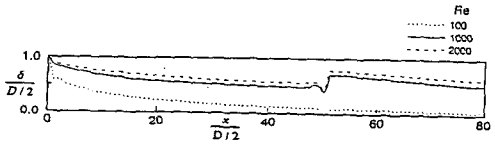

Fig.7 Ice formation layer for various Reynolds numbers in a stenotic tube.

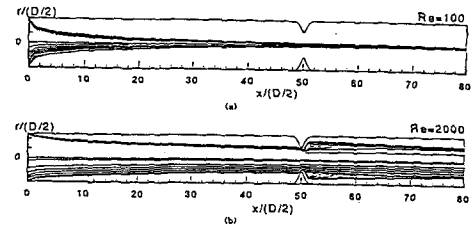

Fig.8 Contour plots for isotherms (upper) and stream lines (lower) : (a) Re = 100, (b) Re = 2000.

similar. for the stenotic port where two cases are The flow and temperature fields are plotted in Fig.8 for both of Re=100 and 2000. For Re=100 depicted in Fig.8(a), it is clear that before the stenotic port both the hydrodynamic and thermal boundary layers start at the tube inlet and are gradually developing in the axial direction, becoming fully developed through the stenotic port. However, the recirculation vortex behind the stenotic port was not observed. The absence of the recirculation vortex leads to the smooth shape of the ice layer behind the stenotic port. Fig.8(b) depicts the flow and temperature fields for Re=2000 and shows that the thermal boundary layer was pushed into the ice layer by the momentum of the higher fluid velocity, therefore the ice layer growth was moderately restrained.

On the other hand, the stretched recirculation vortex just behind the stenotic port is covered over the larger area compared to the lower Reynolds number of Re=1000. Fig.8(b) also shows that most of the isothermal lines are formed in the vicinity of the ice layer and some of them are temporarily separated from the ice wall just behind the stenotic port, then closely adheres to the ice layer far away from the stenotic port. From this behavior for isothermal lines for Re=2000, it can be deduced that the ice layer growth behind the stenotic port is more impeded in a larger area with increasing fluid velocity in a tube. In a investigation, as shown in Fig.9, for the variation of ice layer thickness in a center of stenotic portion with respect to Reynolds number, it is shown that, as Re increases, the ice layer thickness gets thinner monotonically with a trend varied concavely.

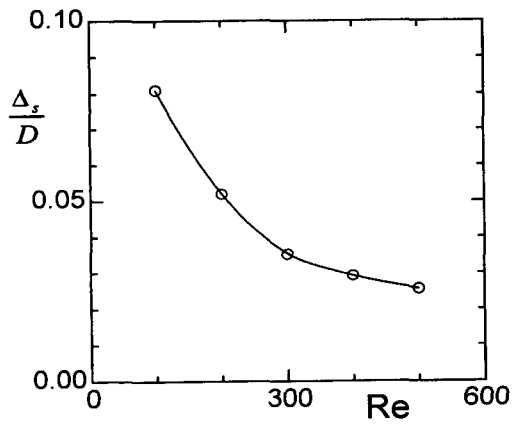

Fig.9 Variation of the ice layer thickness at the center of stenosis with various Reynolds numbers in λ_s= 1.0D and δ_s=0.3D.

3.3 Variation of heat transfer coefficient

The distribution of local Nusselt number Nu is plotted against $\chi/(D/2)$ in Fig.10 for several values of $h/(D/2)$ to investigate the effect of an ice layer thickness on the heat transfer characteristics at the interface. For a straight tube (h=0), Nu monotonically decreases with increasing $\chi/(D/2)$. It is well known from the previous investigations that the monotonic decreasing in Nu results from the increase in thermal resistance along the tube caused by the ice layer growth. On the other hand, the trend for Nu in the stenotic tube is more complex than for the straight tube. The Nu variation is about the same as that of a straight tube before the stenotic port, while Nu suddenly fluctuates near the stenotic port and gradually decreases in the

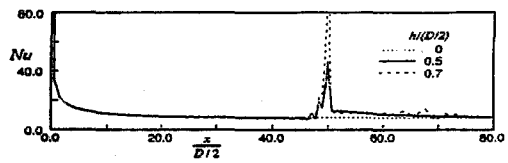

Fig.10 The distribution of the local heat transfer coefficient along the interface of the ice formation for the various heights of stenotic port.

axial direction, approaching asymptotically to that of a straight tube again. Due to the thinner thickness of ice layer behind the stenotic port, the magnitude of *Nu* fluctuation is much more amplified as the height of stenotic port increases. Conclusively, the slight fluctuation of *Nu* is observed far downstream of the stenotic port because of the recirculation cells formed downward of the stenotic port.

4. Conclusion

A numerical analysis is made for the freezing phenomena in stenotic tube for a steady state laminar flow. The present study is markedly different from the existing works in that the complete set of governing equations in both the solid and liquid regions are numerically resolved. Results were obtained for various positions and heights of stenotic shape and flow rates. The ice layer growth monotonically increases in the axial direction for the straight tube, while it experiences the fluctuation of shape through the stenotic port. It is clear that the fluctuation of ice layer shape results from the recirculation vortex of flow which suppresses the ice layer growth. This growth is magnified increasingly in a stenotic height. This phenomenon of the fluctuation of ice layer is more clear as the flow rate increases. It is also found that the local heat transfer coefficient drops exponentially at the inlet of tube, and decreases monotonically before the stenotic port, but experiences fluctuation with the variation of the ice layer thickness. For the higher value of a stenotic height, it is found that some of the fluctuations of local heat transfer coefficient result from the recirculation cells formed downstream of the flow passage.

Acknowledgements

This work was supported by Research Center for Aircraft Technology at Gyeongsang National University and Turbo and Power Machinery Research Center at Seoul National University.

References

(1) Zerkle. R. D. and Sunderland, J. E., 1968, " The Effect of Liquid Solidification in a Tube Upon Laminar-Flow Heat Transfer and Pressure Drop," *J. Heat Transfer*, Trans. ASME, pp. 183-190.

(2) Lee, D. G. and Zerkle, R. D., 1969, "The Effect of Liquid Solidification in a Parallel Plate Channel Upon Laminar-Flow Heat Transfer and Pressure Drop," *J. Heat Transfer*, Trans. ASME, pp. 583-585.

(3) Kikuchi, Y., Shigemasa, Y., Oe, A. and Ogata, T., 1986, "Steady-State Freezing of Liquids in Laminar Flow between Two Parallel Plates," *J. Nucl. Sci. Technol.*, Vol. 23, pp. 979-991.

(4) Suh, J.-S., Ro, S. T. and Kim, M.-G., 1996, "Analysis of Ice-Formation Phenomena in a Stenotic Tube", *Proci. ISTE-CR-5*, Vol. 1, pp. 264-269.

(5) Cho, Chul and Ozisik, M. N., 1979, "Transient Freezing of Liquids in Turbulent Flow inside Tubes," *J. Heat Transfer*, Vol. 103, pp. 363-468.

(6) Gilpin, R. R., 1981, "Ice Formation in a Pipe Containing Flow in the Transition and Turbulent Regimes," *J. Heat Transfer*, Vol. 103, pp. 363-368.

(7) Seki, N., Fukusako, S. and Younan, G. W., 1984, "Ice-Formation Phenomena for Water Flow Between Two Cooled Parallel Plates," *J. Heat Transfer*, Vol. 106, pp.

498-505.

(8) Hirata, T. and Matsuzawa, H., 1987, " A Study of Ice-Formation Phenomena on Freezing of Flowing Water in a Pipe," *J. Heat Transfer*, Vol. 109, pp. 965-970.

(9) Weigand, B. and Beer, H., 1993, "Ice-Formation Phenomena for Water Flow inside a Cooled Parallel Plate Channel: an Experimental and Theoretical Investigation of Wavy Ice Layers," *Int, J. Heat Mass Transfer*, Vol. 36, pp. 685-693.

(10) Patankar, S. V., 1980, *Numerical Heat Transfer and Fluid Flow*, Hemisphere, Washington, DC.

(11) Suh, Jeong-Se and Ro, Sung Tack, 1995, "Close-Contact Melting of Ice in a Horizontal Cylinder," *Trans. KSME*, Vol. 19, pp. 2595-2606.

(12) Karki, K. C. and Patankar, S. V., 1988, "Cal-culation Procedure for Viscous Incompressible Flows in Complex Geometries," *Numer. Heat Transfer*, Vol. 4, pp. 295-307.